RSC Advances

PAPER

View Article Online
View Journal | View Issue

Cite this: *RSC Adv.*, 2020, **10**, 4795

Immobilization of laccase on magnetically separable biochar for highly efficient removal of bisphenol A in water†

Yu Zhang,[a] Mingyue Piao,[ab] Lingzhi He,[a] Lan Yao,[a] Tiezhu Piao,[c] Zairan Liu[a] and Yunxian Piao *[a]

Received 26th October 2019
Accepted 10th January 2020

DOI: 10.1039/c9ra08800h

rsc.li/rsc-advances

Laccase was stably immobilized on a cost effective and nanosized magnetic biochar (L-MBC) by adsorption, precipitation and crosslinking, and it was used for high performance BPA removal. A large amount of enzyme could be immobilized on the magnetic biochar with high activity (2.251 U per mg MBC), and the L-MBC could be magnetically separated from the aqueous solution in 20 seconds. The successful immobilization of laccase was also confirmed *via* FTIR, SEM, and EDS analyses. The L-MBC presented better storage and stability performances, pH tolerance and thermal stability than the free laccase. It was found that BPA with an initial concentration of 25 mg L^{-1} could be thoroughly removed within 75 min, where BPA removal was attributed to enzymatic degradation and adsorption. In addition, the BPA removal efficiency by the L-MBC could be maintained above 85% even after seven cycles of repeated use. Due to high stability and efficient recyclability, the L-MBC-based biocatalyst has the potential to be a reliable method for treating BPA in environmental water sources.

1. Introduction

In recent years, exogenous estrogens as a kind of endocrine disrupting chemicals (EDCs) such as pesticides, industrial compounds, and chemical products have often been detected in various environmental media.[1] Among them, BPA is mostly detected because of its extensive industrial applications and the tremendous amount of global production.[2–4] BPA is released into the water sources through municipal wastewater, which can lead to bioaccumulation in miscellaneous food chains, ultimately endangering human health and causing diseases such as testicular and prostate cancer.[5] In this sense, the development of reliable methods for the highly efficient removal of the BPA contaminant is urgently needed.

Until now, various methods have been utilized for the removal of BPA such as adsorption, photocatalytic degradation, biodegradation, and advanced oxidation.[5–9] Among them, the enzyme biocatalytic method is attractive due to advantages such as the high efficiency of the reaction, simplicity in operation, and low toxicity.[10] Laccase, a kind of oxidoreductase, is a favorable enzyme for the removal of BPA because only oxygen is needed as an electron acceptor during the reaction rather than other additional reagents such as hydrogen peroxide or divalent manganese.[11] However, it is well known that free laccase has poor stability and is difficult to reuse, which limits its practical applications. Thus, it is critical to improve the stability and reusability of enzymes. Enzyme immobilization is known as one of the reliable methods for meeting requirements including stability, and easy separation.[12] Various methods of laccase immobilization on nanomaterials, membranes, and fibers[13–15] have been accessed by either adsorption, encapsulation, or covalent binding.[12,16,17] However, the development of low cost and environmentally friendly nanomaterials based on stable nanobiocatalysts for the efficient removal of pollutants is still needed.

Biochar, a carbon material obtained from the pyrolysis of biomass under anaerobic conditions, has advantageous features, such as a large specific surface area, good dispersibility and biocompatibility, for stable and high-load enzyme immobilization.[18,19] Worldwide, the most attractive benefits of biochar compared to other reported materials are its extremely low cost and ubiquitous sources,[20] which would enable highly cost effective nanobiocatalyst construction. To date, biochar has been broadly utilized in the areas of adsorption and soil adaptation and to some extent in fuel cells and sensors.[21–24] However, the research on the biochar as a matrix for stable enzyme immobilization and utilization for pollutant removal has not been extensively accessed. In this sense,

[a]*Key Laboratory of Groundwater Resources and Environment (Jilin University), Ministry of Education, Jilin Provincial Key Laboratory of Water Resources and Environment, College of New Energy and Environment, Jilin University, 2519 Jiefang Road, Changchun 130021, China. E-mail: yxpiao@jlu.edu.cn*

[b]*College of Environmental Science and Engineering, Jilin Normal University, Siping, Jilin, 136000, China*

[c]*Department of Biological and Chemical Engineering, Yanbian University of Science and Technology, Yanji 133000, China*

† Electronic supplementary information (ESI) available. See DOI: 10.1039/c9ra08800h

investigations on the construction of magnetically separable and stable nanobiocatalysts with nanometer sized biochar are challenging and have significant value in the development of highly cost effective and robust platforms for pollutant removal in complicated environments.

In this study, nanometer sized biochar was first prepared using bagasse and after modification, its surface was modified with magnetic nanoparticles *via* the coprecipitation method. The magnetically separable magnetic biochar (MBC) nanoparticles were utilized for stable enzyme immobilization. Then, laccase was immobilized on MBC (L-MBC) by adsorption followed by precipitation with ammonium sulfate and cross-linking with glutaraldehyde (Scheme 1). The as-synthesized nanobiocatalyst, L-MBC, would have a relatively large amount of enzyme loading and also have good stability due to the cross linking of each enzyme molecule and the well maintained enzymatic activity by the biochar. These characteristics would contribute to high BPA removal performance and easy and efficient reusability.

2. Materials and methods

2.1 Chemicals and apparatus

Laccase (from *Trametes versicolor*), 2,2′-azino-bis(3-ethylbenzothiazoline-6-sulfonic acid) (ABTS), bisphenol A (BPA), glutaraldehyde (GA), ammonium sulfate, and Tris–HCl were purchased from Sigma-Aldrich (St. Louis., MO, USA). Na_2HPO_4, NaH_2PO_4 and citric acid were purchased from Sinopharm Chemical Reagent Co., Ltd (Beijing, China) for the phosphate buffer solution (PBS) and citric phosphate buffer (50 mM) preparation. Ultrapure water (resistivity = 18.25 MΩ cm^{-1}) was used throughout the experiments. All other chemicals and reagents were of analytical grade and used without further purification.

The morphological features of MBC and L-MBC were observed by scanning electron microscopy (XL-30 ESEM FEG Scanning Electron Microscope FEI Company, USA) and energy dispersive spectrometry (Oxford-instruments X-Max, UK). Infrared spectra were obtained using a Fourier transform infrared spectrometer (Nicolet is5, Thermo Fisher, USA).

2.2 Synthesis of magnetic biochar nanoparticles

Magnetic biochar (MBC) nanoparticles were prepared using methods previously reported by our laboratory.[23] Briefly, bagasse was pyrolyzed at 300 °C for 60 min under nitrogen-filled conditions, while maintaining the rate of temperature increase at 7 °C min^{-1} in a tubular furnace (OTF-1200X, Hefei Kejing Materials Technology Co., Ltd. China). Then, biochar particles were prepared by grinding at 300 rpm using a planetary ball mill (YXQM-2L, Changsha Miqi Instrument Equipment Co., Ltd. China). Next, the biochar was dispersed in double distilled water and centrifuged at 5000 rpm for 3 min. The supernatant was dehydrated to obtain biochar nanoparticles (BCNPs). The magnetic biochar nanoparticles were synthesized by adding $FeCl_3 \cdot 6H_2O$, $FeSO_4 \cdot 7H_2O$ and $NH_3 \cdot H_2O$ to the biochar solution at a temperature of 70 °C while purging with nitrogen. Finally, the magnetic biochar nanoparticles were thoroughly washed with double distilled water using magnet separation.

2.3 Immobilization of laccase on magnetic biochar nanoparticle

For stable immobilization of the laccase enzyme on the magnetic biochar nanoparticles (MBCs), laccase (6.5 g L^{-1}) was first incubated in PB solution (50 mM, pH 7.0) containing

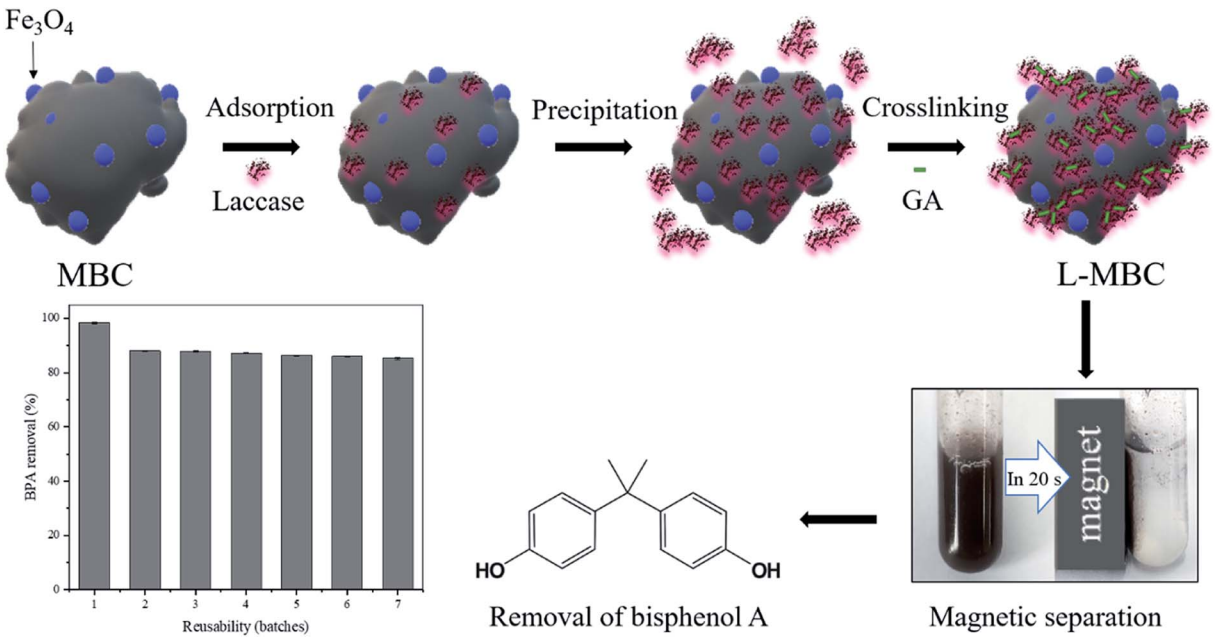

Scheme 1 Schematic for the preparation of L-MBC, digital image of magnetically separated L-MBC, and graph of L-MBC reusability.

magnetic biochar nanoparticles (0.5 g L^{-1}) for 0.5 h at 4 °C with shaking (100 rpm), followed by the addition of ammonium sulfate (final concentration of 300 g L^{-1}) for precipitation of the enzymes. After 0.5 h of the precipitation treatment, GA (final concentration 0.5 wt%) was added for cross linking the enzymes and followed by incubation overnight at 4 °C under dark conditions. Finally, the produced laccase-immobilized MBC (L-MBC) was blocked with Tris–HCl (100 mM, pH 7.4) for 1 h and after thorough washing of excessive reagents, it was stored at 4 °C for further use. The amount of enzyme loading was estimated by elemental analysis of nitrogen in the L-MBC using an elemental analyzer (Elementar vario MICRO cube, Germany).

2.4 Activity and stability of L-MBC

ABTS is a suitable substrate to determine the activity of laccase because ABTS can be oxidized by the catalytic reaction with laccase to generate spectrophotometrically measurable cation radicals ($ABTS^+$).[25–27] Additionally, 1 unit (U) of laccase activity was defined as the amount of laccase that can convert 1 μmol of ABTS into 50 mM of citric phosphate buffer per minute at 25 °C. The activities of free or immobilized laccase were obtained by incubating a specific amount of laccase or L-MBC in 1 μmol of ABTS in 50 mM of citric phosphate buffer for 3 min at 25 °C, and the increase in the absorbance at 420 nm was measured using a UV-vis spectrophotometer (Shimadzu UV-2450, Tokyo, Japan). Enzyme activity was calculated according to the following equations:

$$\text{Free enzyme activity } \left(\text{U g}^{-1}\right) = \frac{\Delta A \times 10^6 \times V_t}{\varepsilon \times \Delta T \times m_1} \quad (1)$$

$$\text{Immobilized enzyme activity } \left(\text{U g}^{-1}\right) = \frac{\Delta A \times 10^6 \times V_t}{\varepsilon \times \Delta T \times m_2} \quad (2)$$

where, ΔA represents the increase in absorbance of $ABTS^+$, V_t represents the volume of the reaction system (L), ε represents the molar extinction coefficient of $ABTS^+$ (36 000 L M^{-1} cm^{-1}), ΔT represents the reaction time (min), m_1 represents the amount of free laccase (g), and m_2 represents the amount of immobilized laccase (g).

To evaluate the stability at different pH values, free laccase and L-MBC were placed in PBS at different pH values, and the residual activities were measured after 2 h of continuous shaking (100 rpm) at room temperature. To measure the storage stability of the L-MBC samples, the samples were stored in PBS and protected from light at 4 °C and 25 °C. Then, the residual activities were measured periodically.

2.5 Removal of BPA

BPA removal experiments using L-MBC were all performed in triplicate at room temperature. Briefly, L-MBC at a concentration of 0.3 g L^{-1} was used to remove BPA (concentrations of 25, 50, and 100 mg L^{-1}) with shaking at 100 rpm. The solution was sampled at specific time intervals, followed by magnetic separation. Additionally, the concentration of BPA in the supernatant was measured. The concentration of BPA was determined using high performance liquid chromatography (LC-20AT HPLC system, Shimadzu, Japan) equipped with an Eclipse Plus C18 column (250 mm × 4.6 mm, particle size of 5 μm, Agilent, Palo Alto, CA, USA). The mobile phase was a mixture of acetonitrile and ultrapure water (50 : 50) with a flow rate of 1.0 mL min^{-1} at 30 °C. BPA was detected by absorbance at 278 nm using a UV-vis detector with a retention time of 6.5 min.

To investigate the amount of BPA that was converted by the catalytic reaction of laccase, the amount of BPA adsorbed onto the L-MBC conjugate was quantified after the desorption of BPA using pure methanol with ultrasound for 20 min. Additionally, the portion of degraded BPA was calculated by subtraction of the concentration of the adsorbed portion from the concentration of the total amount removed.

Moreover, in order to explain the removal mechanism of L-MBC, BPA removal was also performed with deactivated L-MBC under the same conditions. The deactivated L-MBC was prepared by incubating a solution of L-MBC at 80 °C for 2 h.

Compounds produced from BPA degradation with L-MBC were analyzed using gas chromatograph-mass spectrometry (GC-MS) (Agilent 6890/5973, USA). For the analysis, the pH of the reaction mixture after 90 min of BPA degradation was adjusted to 2.0 with 1 M HCl, and the compounds were extracted with dichloromethane three times with vigorous shaking and concentrated to 1 mL using a nitrogen blowing device. A DB-5 column was used as the chromatographic column. During GC, nitrogen was used as the carrier gas at a constant flow rate of 1.5 mL min^{-1}. With respect to the temperature rising program, the initial temperature (50 °C) was maintained for 2 min, and then increased to 100 °C at a rate of 6 °C min^{-1}. Next, the temperature was increased to 280 °C at a rate of 10 °C min^{-1}, and this temperature was held for 5 min. The temperature of the injector and detector were 250 °C and 280 °C, respectively. Mass spectra were recorded in the electron ionization mode with an ion source temperature of 230 °C and electron bombardment energy of 70 eV at a scanning range of 40–700 *m*/*z*.

2.6 Reusability of L-MBC and environmental water remediation

The reusability of L-MBC was investigated by evaluating the removal efficiency of BPA by treating fresh BPA solutions for seven cycles. Every experiment was performed in triplicate. In each cycle, 0.7 g L^{-1} of L-MBC was reacted with 25 mg L^{-1} of BPA at 25 °C for 60 min.

To investigate the practicability of L-MBC for the removal of BPA in real environmental water sources, water samples from the upper reaches of the Yitong River, Changchun, China were taken. The water sample was spiked with 25 mg L^{-1} of BPA, and the pH was adjusted to 5.5. Then, BPA was treated using 0.3 g L^{-1} of L-MBC at room temperature for 2 h. All the measurements were performed in triplicate.

3. Results and discussion

3.1 Characteristics of L-MBC

The magnetically separable and highly stable nanobiocatalyst, L-MBC, was prepared by immobilizing the laccase enzyme on

the magnetic biochar (MBC) nanoparticles using processes of adsorption, precipitation and crosslinking. First, laccase was adsorbed onto MBC by simple physical adsorption. Then, soluble laccase precipitated near the MBC under high salinity conditions, increasing the chance of contact and adsorption on the MBC. Finally, by treating with glutaraldehyde, a large amount of the precipitated laccase would be crosslinked and immobilized on the MBC (Scheme 1).

The physical and chemical properties of L-MBC were first investigated. As shown in Fig. 1a, the SEM images indicated that a large number of magnetic nanoparticles were synthesized on the biochar particles by co-precipitation. The presence of magnetic nanoparticles was also confirmed by the elemental mapping image in Fig. S1,† where the iron element was distributed on the biochar surface. The produced L-MBC could be separated from the solution in 20 s *via* external magnetic force, which is favorable for the separation of the nano-biocatalyst after the removal of the pollutant.

As shown in Fig. 1b, after enzyme immobilization on the MBC with adsorption and precipitation, a smooth looking and lightly layered enzyme coating appears on the surface of the MBC. Additionally, with a further crosslinking process, a heavily layered enzyme coating was produced on the surface of the MBC (Fig. 1c), which made the surface of the L-MBC smoother. As shown in Fig. 1d, in the upper left corner of the locally magnified image of the L-MBC, a film-like morphology can be clearly seen, which was formed from a large amount of laccase aggregates produced on the MBC by adsorption, precipitation and cross linking. As shown in the elemental mapping in Fig. S2,† the distinct shape that appeared in the mapping diagrams of nitrogen and sulfur also demonstrated the successful immobilization of the enzyme proteins.

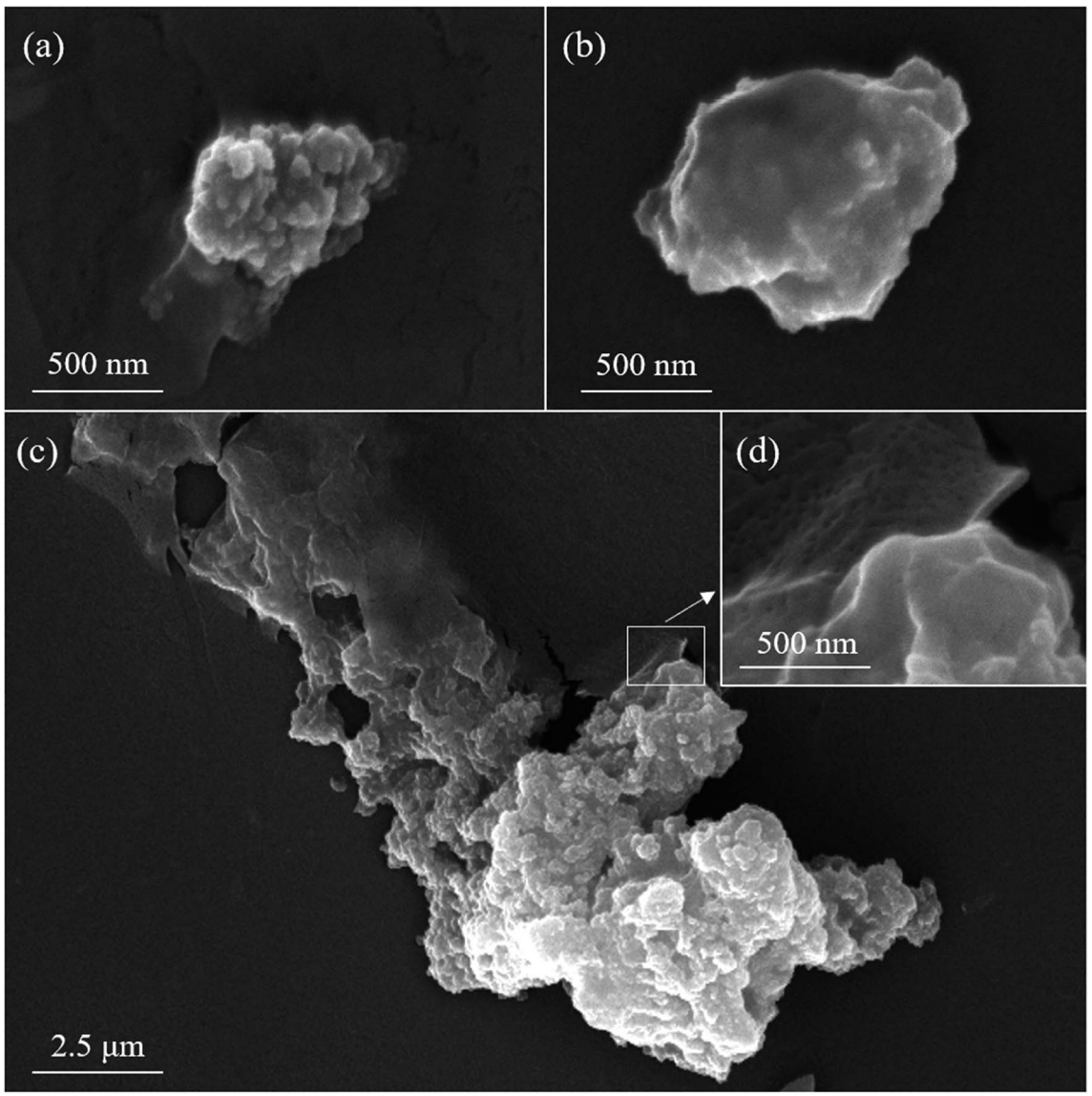

Fig. 1 Scanning electron microscope images of (a) magnetic biochar (MBC), (b) L-MBC prepared by adsorption and precipitation of laccase, (c) L-MBC prepared by adsorption, precipitation and crosslinking of laccase, and (d) zoomed in image of (c).

The characteristics of L-MBC were also investigated using Fourier transform infrared (FTIR) analysis. As indicated in Fig. 2, the absorption peaks at 593 and 581 cm^{-1} were due to the vibrations of the Fe–O bond, indicating the successful loading of the magnetic nanoparticles. The peaks at 1050 and 1071 cm^{-1} represented the C–H bonds of the aromatic rings in biochar,[28] while the sharp peak at 1026 cm^{-1} was assigned to the stretching vibration of C–O from the laccases,[29] which resulted in a broad peak of L-MBC at 1059 cm^{-1} because of the immobilization of laccase. The broad absorption peaks at 1626–1641 cm^{-1} may be related to the stretching vibration of the C═O bond from the carboxyl group in biochar and the amide bond existing in the laccase protein. The bands at around 2924 cm^{-1} corresponding to asymmetric C–H and symmetric C–H vibrations were due to alkyl groups such as $–CH_2$ and $–CH_3$. Additionally, hydroxyl stretching vibrations were observed at 3420–3442 cm^{-1}. The FTIR analysis also confirmed the successful preparation of magnetic biochar loaded with laccase.

3.2 Activity of L-MBC

The enzyme loading amount and specific activity of L-MBC were evaluated. As shown in Table 1, after the precipitation process, the enzyme loading increased from 0.027 mg_{Lac} mg_{MBC}^{-1} to 0.048 mg_{Lac} mg_{MBC}^{-1}. The nearly two-fold increase indicates that precipitation can increase the enzyme loading directly through the physical process. After crosslinking, a large amount of enzymes was immobilized onto the MBC (1.424 mg_{Lac} mg_{MBC}^{-1}), due to which the enzyme loading increased by 30-fold. The enzyme loading was also higher than that found in recent studies on the immobilization of laccase onto different carbon materials such as Fe_3O_4@GO (0.145 mg mg^{-1}),[8] pristine few layer graphene (0.221 mg mg^{-1}),[30] amine-functionalized Fe_3O_4@C nanoparticles (0.195 mg mg^{-1}),[31] and PEI/CNT (0.556 mg mg^{-1}).[32] Meanwhile, laccase activity per mg of MBC supporter was up to 2.251 U, which is higher than that obtained from adsorption or the combined adsorption and precipitation method. Additionally, this is superior to others reports, such as that by Lonappan *et al.* who achieved 0.031 U per mg of pig manure biochar using the adsorption immobilization[33] and Naghdi *et al.* who achieved 0.005 U per mg of pinewood nanobiochar by covalent immobilization.[34] This result confirmed that crosslinking after precipitation was very effective for the immobilization of the enzyme because of high degree of enzyme crosslinking. It was also found that the specific activity of L-MBC was not significantly reduced by the precipitation and crosslinking processes (1.581 U mg_{Lac}^{-1}) in comparison to that by simple adsorption (1.672 U mg_{Lac}^{-1}), suggesting that the enzymes were effectively immobilized on the MBC in three steps.

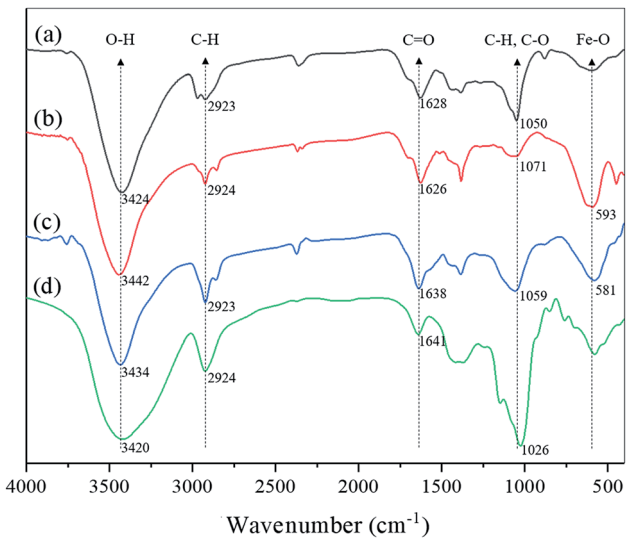

Fig. 2 FTIR spectra of (a) biochar, (b) MBC, (c) L-MBC, and (d) laccase.

3.3 Stability of L-MBC

For practical applications, it is critical for biocatalysts to have good stability. The stabilities of free laccase and L-MBC at 50 mM in PBS at various pH values (4–8) were studied *via* incubation at 25 °C with shaking (100 rpm). As shown in Fig. 3a, after 2 h of continuous shaking, the relative activities of the free laccase were reduced to 36.4%, 42.1%, 61.9%, 68.4%, and 34.6% at pH of 4, 5, 6, 7, and 8, respectively. Nevertheless, the residual activities of the immobilized enzyme were maintained at 83.5%, 92.6%, 94.8%, 95.2%, and 91.5%, correspondingly, suggesting that the stability of immobilized laccase at different pH values was higher than that of free laccase. In addition, it was also found that both free and immobilized enzymes presented optimum stability at pH 7.

Furthermore, the long term stability of L-MBC at 4 °C and 25 °C was also investigated. As shown in Fig. 3b, after 30 days of storage, the residual activities of L-MBC at 4 °C and 25 °C were maintained at 81.8% and 64.4%, respectively. In contrast, the residual activities of free laccase after 30 days at 4 °C and 25 °C were 54.2% and 35.5%, respectively. It is worth mentioning that L-MBC still retained more than 90% of its relative activity after 18 days of storage at 4 °C and 7 days after storage at 25 °C. These results suggested that the storage stability of the immobilized laccase on MBC was superior compared to that of free laccase. This might be due to the fact that when laccase was crosslinked and adsorbed onto the magnetic biochar, the molecular conformational mobility of laccase was limited, making it less susceptible to denaturation,[35,36] which would provide more possibilities for the practical application of L-MBC.

The pH of the solution may change the ionization state of the amino acids in the enzyme and affect its structure and activity, and even lead to its denaturation.[37,38] Hence, the activity profiles of free laccase and laccase immobilized on MBC were investigated by performing activity assays at different pH values. As shown in Fig. 4a, free and immobilized laccases exhibited the greatest activity at pH 3 and 3.5, which is probably due to the limited mobility of laccase due to ionic interactions between the enzyme and MBC.[39–41] Hence, in the subsequent experiments, the activity assays were all performed at pH 3.5. It was also found that the laccase immobilized on MBC had a broader range of working pH values when compared to the free laccase, suggesting that L-MBC was more favorable than free laccase at various pH conditions.

Table 1 A comparison of enzyme loading and activity of immobilized laccase on the MBC prepared by adsorption, precipitation and crosslinking methods (pH = 3.5, 25 °C)

	Adsorption	Adsorption & precipitation	Adsorption, precipitation & crosslinking
Laccase loading (mg Lac per mg MBC)	0.027	0.048	1.424
Activity per MBC (U per mg MBC)	0.045	0.082	2.251
Specific activity (U per mg protein)	1.672	1.719	1.581

The activity profiles of L-MBC at different temperatures were also investigated. As shown in Fig. 4b, free laccase showed the highest enzyme activity at 40 °C, while the optimal activity of the immobilized laccase occurred at 45 °C. Compared with free laccase, the L-MBC presented higher activity even at high temperatures of 50 °C, 55 °C, 60 °C, and 65 °C, with relative enzyme activities of 77.3%, 70.4%, 55.5%, and 45.5%, respectively. It was also noted that some enzymatic activity remained (19.5%) at the extreme condition of 70 °C. This might be due to the multipoint attachment between the enzyme molecules and the magnetic biochar and also the increased diffusion ability of the substrate at higher temperatures.[34,42] This also suggested that magnetic biochar can help maintain the activity of laccase, probably because MBC as a carrier can protect the conformational structure of laccase under different environmental conditions.[43]

3.4 Removal of BPA

The efficiencies of BPA removal with L-MBC at different pH were investigated. As shown in Fig. 5a, L-MBC presented a very good

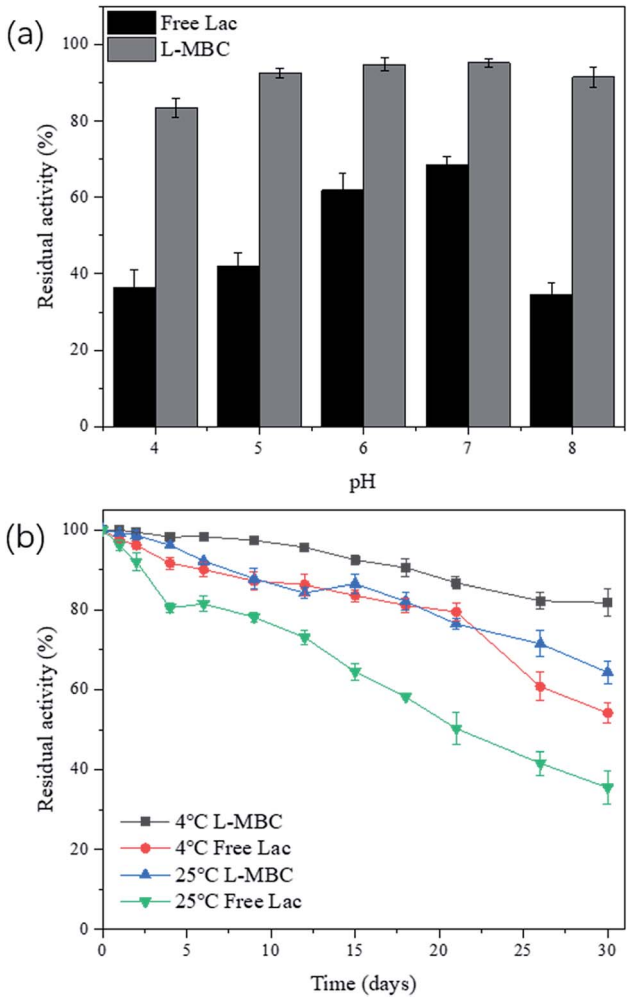

Fig. 3 Stability profiles of L-MBC and free laccase. (a) Residual enzyme activities after incubating in PB solution with various pH values under continuous shaking (100 rpm) for 2 h and (b) residual enzyme activities after storage at 4 °C and 25 °C in PB solution (pH = 7.0).

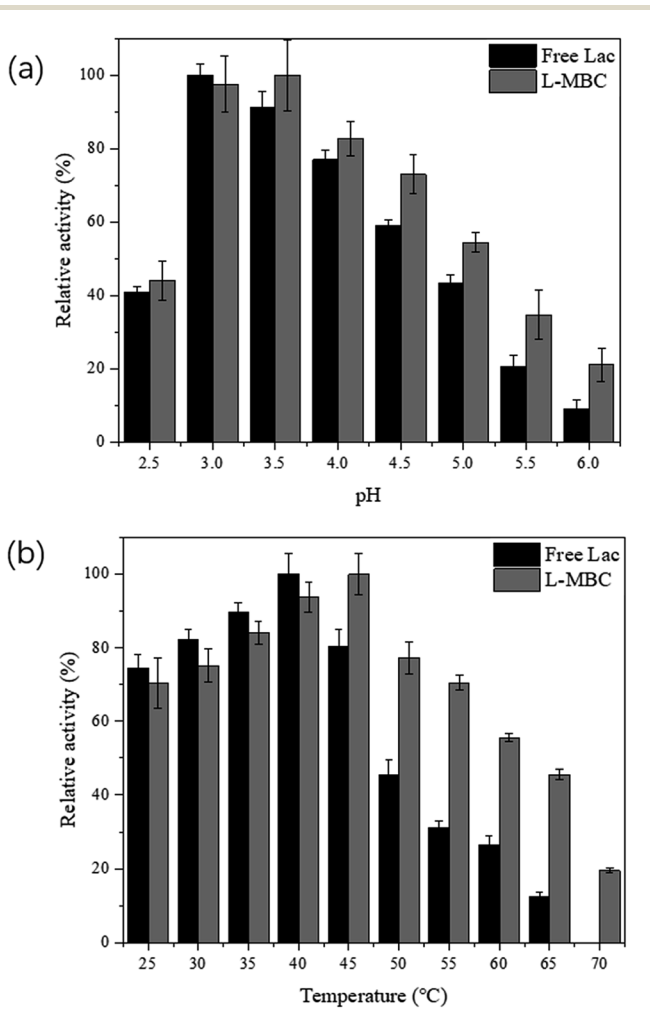

Fig. 4 Relative activity profiles of free laccase and L-MBC measured at various (a) pH and (b) temperatures.

performance in the removal of BPA at pH 3.5, and BPA can be completely removed in 75 min. At pH 4.5 and 5.5, the removal efficiencies of BPA after 90 min can reach 98.99% and 84.18%, respectively. By analyzing the amount of BPA desorbed from the L-MBC after 90 min, the amounts of adsorbed and degraded BPA were evaluated. As indicated in Fig. 5b, the percentages of BPA degradation by immobilized laccase reached 31.46%, 42.93%, and 46.97% at pH 3.5, 4.5, and 5.5, respectively. Therefore, at pH 5.5, the immobilized laccase had the highest degradation ability toward BPA. Additionally, the percentages of BPA adsorbed on L-MBC were 68.54%, 56.05%, and 37.21%, correspondingly. In one point of view, the isoelectric point of laccase from *Trametes versicolor* is 5.68,[44] so laccase should be positively charged in the acidic solution, which would lead to electrostatic adsorption of negatively charged BPA. On the other hand, the adsorption of BPA by L-MBC may be due to H-bonding interactions occurring between MBC and BPA.[23] Such adsorption would be helpful for the affinity of the immobilized enzymes for fast and efficient targeted BPA degradation. Moreover, because of the pK_a value of BPA (9.6–10.2),[45] in a solution of lower pH, a small portion of BPA may also be absorbed onto the biochar in L-MBC through protonation or cation exchange. As the pH increases, the partition coefficient of BPA would decrease and result in a reduction in the adsorption efficiency.

The effect of initial BPA concentration on the removal efficiency of BPA by L-MBC was investigated. As shown in Fig. 5c, when the initial concentrations of BPA were 25, 50, and 100 mg L^{-1}, the BPA removal efficiencies after 90 min reached 100%, 97.89%, and 84.87%, respectively. It is worth mentioning that when the initial concentration of BPA was 50 mg L^{-1}, the removal efficiency at 60 min exceeded 90%, which indicated that L-MBC can also perform well in aqueous solutions with a high concentration of pollutants. However, the removal rate of BPA decreased with increment in the initial BPA concentrations, which might be because a high initial concentration of BPA can exceed L-MBC's processing capacity. As shown in Fig. 5d, the percentage of BPA degradation by immobilized laccase increased from 31.46% to 45.36% and 63.46% as the initial BPA concentrations elevated from 25 mg L^{-1} to 50 mg L^{-1} and 100 mg L^{-1}, respectively. Additionally, the percentages of BPA adsorption on L-MBC decreased from 68.54% to 52.52% and 21.41%, correspondingly. This result may be because the initial concentration determines the amount of contact between the reactant molecules and the enzyme active sites, and it can provide the molecules with a driving force to resist mass transfer resistance between the aqueous and solid phases.[29]

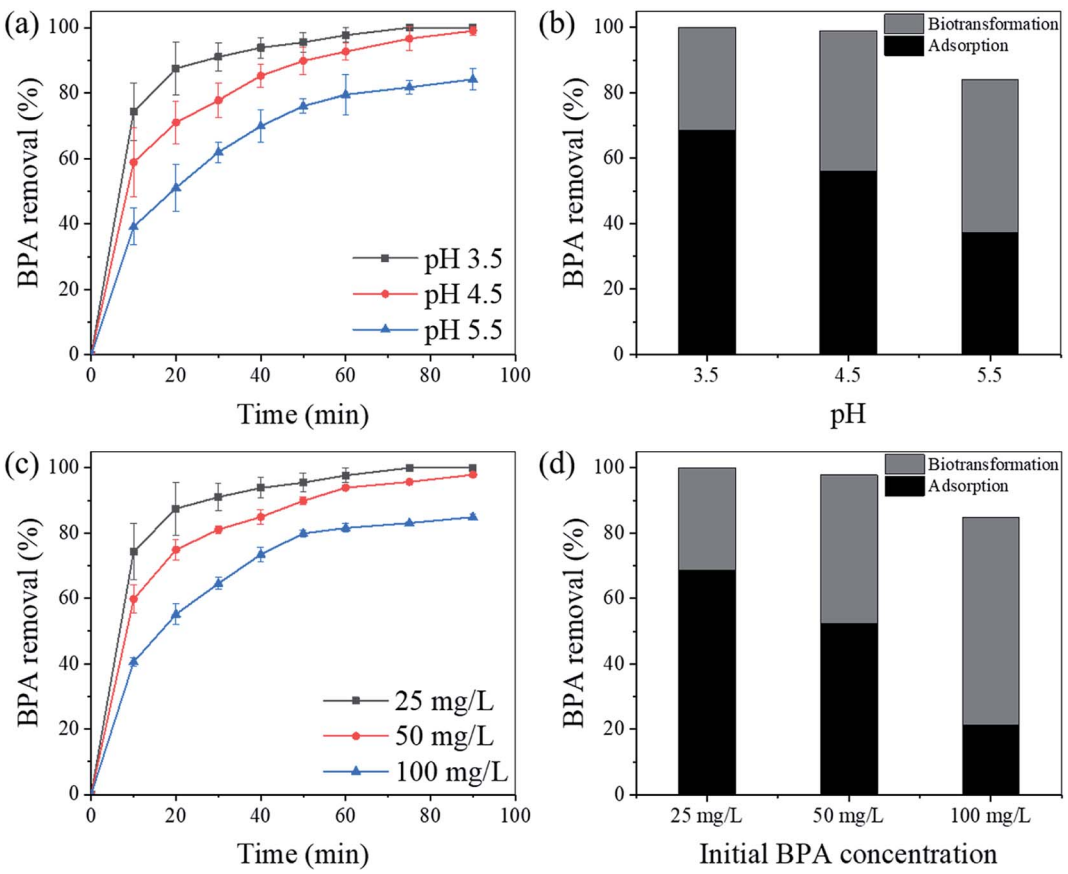

Fig. 5 (a) BPA removal profiles at different pH values (L-MBC 0.3 g L^{-1} and BPA 25 mg L^{-1}), (b) percentages of biotransformation and adsorption after 90 min of reaction time in correspondence with (a), (c) BPA removal profiles at different initial BPA concentrations (L-MBC 0.3 g L^{-1}, pH = 3.5), and (d) percentages of biotransformation and adsorption after 90 min of reaction time in correspondence with (c).

Interestingly, the degradation efficiencies at high initial concentrations of BPA (50 and 100 mg L^{-1}) remained high, indicating that the immobilized laccase has potential to be utilized even at high substrate concentrations.

In an attempt to explain the mechanism of how L-MBC removes BPA, the corresponding BPA removal profiles with deactivated L-MBC were compared (Fig. S4†). We speculated that during BPA removal, adsorption and the enzymatic turn over reaction both exist, and the enzymatic reaction should be dominant and the adsorption process may contribute to the fast and easy mass transfer.

The compounds produced by BPA removal with L-MBC were also evaluated by using GC-MS analysis. Table S1† lists the retention times and possible metabolites. The degradation pathways showing how the degradation products could be generated are indicated in Fig. S5.† First, C–C bonds, the most vulnerable in BPA, are cleaved by the catalytic reaction of laccase to form 2,4-di-*tert*-butylphenol and 4-isopropenylphenol.[46] 4-Isopropenylphenol, although not detected, has previously been reported as a product of the oxidation of BPA.[47,48] Then, 2,4-di-*tert*-butylphenol could continue to be oxidized to 2,4-dimethylbenzaldehyde and 4-isopropenylphenol could be converted to phenol, hydroquinone, and 2,4-dimethylbenzaldehyde.[15] Finally, tartaric acid and 3-methylbutanoic acid might be formed following oxidation reactions and the ring fusion of aromatics.[3,25] Through the analysis of the degradation products, we found that the toxicity of the products was significantly lower than that of the original substrates.

3.5 Reusability of L-MBC for BPA removal and environmental water remediation

Considering the cost effectiveness of the pollutant treating process, it is worth evaluating the reusability of L-MBC. As shown in Fig. 6, after seven BPA removal cycles, the removal efficiency of L-MBC was still maintained at over 85%. After two reuses, the removal efficiency dropped to 88.05%, which was probably due to minor enzyme detachment. Additionally, the BPA removal efficiency was slightly lowered after each sequential reuse, which may be caused by the inhibition effect of the by-products on the immobilized enzyme.[49] In terms of the low operation cost and comparable removal efficiency, this reusable immobilized laccase on MBC with fast magnetic separation ability has great prospects for the remediation of BPA polluted water.

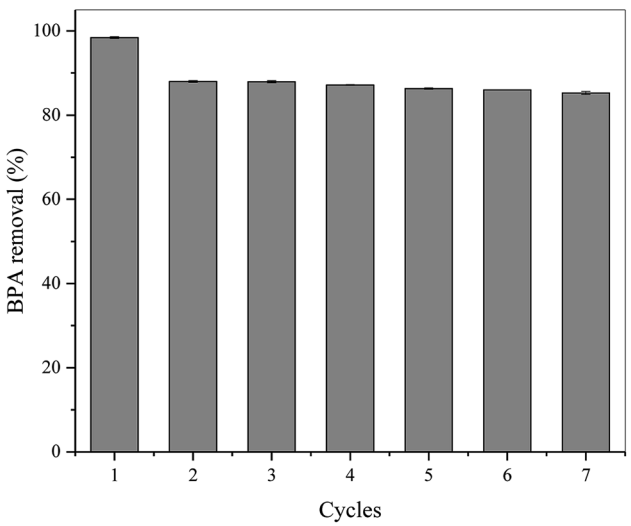

Fig. 6 Reusability of L-MBC (0.7 g L^{-1}) towards the removal of BPA (25 mg L^{-1}) (pH = 5.5, T = 25 °C, t = 1 h).

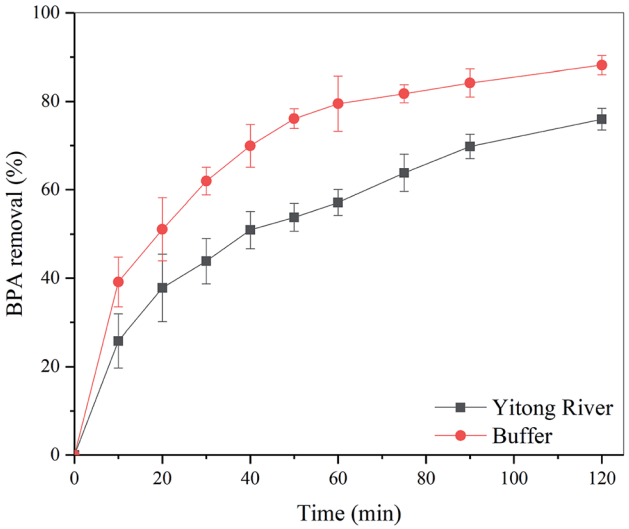

Fig. 7 Comparison of the BPA (25 mg L^{-1}) removal profiles performed in environmental water and buffer using L-MBC (0.3 g L^{-1}) (pH = 5.5, T = 25 °C, t = 2 h).

To investigate the possibility of the practical application of L-MBC, real environmental water samples were collected from the Yitong River, Changchun (the concentrations of the main ions are shown in Table S2†). As the only transiting river in Changchun, the Yitong River is the main drainage river in Changchun, which usually contains about 80% of the industrial wastewater and domestic sewage. After spiking with BPA, the removal profile using L-MBC was evaluated. As shown in Fig. 7, after a 2 h treatment, the removal efficiency of BPA reached above 75%, which is 12.82% lower than that under buffer conditions. The slightly reduced BPA removal ability is possibly due to the effect of some interfering ions and substances contained in the water samples. The results indicated that L-MBC has the potential to be used in the actual water treatment of BPA.

4. Conclusions

In conclusion, laccase was stably immobilized on magnetic biochar nanoparticles by adsorption, precipitation and cross-linking methods, and was successfully utilized for the efficient removal of BPA. A large amount of laccase immobilization on the MBC could be confirmed by SEM, EDS and FTIR analysis. L-MBC was proved to have higher enzyme activity when compared with free laccase over a broad range of pH and temperature conditions. Through comparative analysis of BPA removal under different conditions and analysis of the produced

compounds, it was clarified that the mechanism of BPA removal with L-MBC was by both enzymatic conversion and adsorption, and the toxicity of the product was substantially reduced. L-MBC was also demonstrated to have good stability, easy magnetic separation ability and reusability, which would provide a robust platform for the efficient treatment of BPA pollutant in environmental water sources.

Conflicts of interest

There are no conflicts to declare.

Acknowledgements

This study was financially supported by the National Natural Science Foundation of China (51809111) and the open fund from the Key Lab of Eco-restoration of Regional Contaminated Environment (Shenyang University), Ministry of Education (2019_ERRCE_K2).

References

1 M. Bilal, H. M. N. Iqbal and D. Barcelo, *Sci. Total Environ.*, 2019, **689**, 160–177.
2 A. Cydzik-Kwiatkowska, K. Bernat, M. Zielińska, K. Bułkowska and I. Wojnowska-Baryła, *Int. Biodeterior. Biodegrad.*, 2017, **122**, 1–11.
3 D. Daâssi, A. Prieto, H. Zouari-Mechichi, M. J. Martínez, M. Nasri and T. Mechichi, *Int. Biodeterior. Biodegrad.*, 2016, **110**, 181–188.
4 L. M. Divya, G. K. Prasanth, K. G. Arun and C. Sadasivan, *Int. Biodeterior. Biodegrad.*, 2018, **135**, 19–23.
5 C. Barrios-Estrada, M. J. Rostro-Alanis, A. L. Parra, M. P. Belleville, J. Sanchez-Marcano, H. M. N. Iqbal and R. Parra-Saldivar, *Int. J. Biol. Macromol.*, 2018, **108**, 837–844.
6 L. N. Nguyen, F. I. Hai, W. E. Price, F. D. L. Leusch, F. Roddick, E. J. McAdam, S. F. Magram and L. D. Nghiem, *Int. Biodeterior. Biodegrad.*, 2014, **95**, 25–32.
7 J. Sharma, I. M. Mishra and V. Kumar, *J. Environ. Manage.*, 2015, **156**, 266–275.
8 W. Qiao and H. Liu, *Int. J. Biol. Macromol.*, 2019, **138**, 1–12.
9 Z. Sun, L. Zhao, C. Liu, Y. Zhen and J. Ma, *Chem. Eng. J.*, 2020, **381**, 122510.
10 W.-J. Xu, Y.-K. Huang, F. Li, D.-D. Wang, M.-N. Yin, M. Wang and Z.-N. Xia, *Biochem. Eng. J.*, 2018, **138**, 37–46.
11 J. Berrio, F. J. Plou, A. Ballesteros, Á. T. Martínez and M. J. Martínez, *Biocatal. Biotransform.*, 2009, **25**, 130–134.
12 T. Brugnari, M. G. Pereira, G. A. Bubna, E. N. de Freitas, A. G. Contato, R. C. G. Correa, R. Castoldi, C. G. M. de Souza, M. Polizeli, A. Bracht and R. M. Peralta, *Sci. Total Environ.*, 2018, **634**, 1346–1351.
13 Z. Zhu, Z. Chen, X. Luo, W. Liang, S. Li, J. He, W. Zhang, T. Hao and Z. Yang, *Chemosphere*, 2020, **240**, 124882.
14 N. A. Samak, Y. Tan, K. Sui, T.-T. Xia, K. Wang, C. Guo and C. Liu, *Mol. Catal.*, 2018, **445**, 269–278.
15 R. Das, G. Li, B. Mai and T. An, *Sci. Total Environ.*, 2018, **640–641**, 798–806.
16 S. Kashefi, S. M. Borghei and N. M. Mahmoodi, *J. Mol. Liq.*, 2019, **276**, 153–162.
17 M. Piao, D. Zou, Y. Yang, X. Ren, C. Qin and Y. Piao, *Materials*, 2019, **12**, 704.
18 Y. Liu, L. Lonappan, S. K. Brar and S. Yang, *Sci. Total Environ.*, 2018, **645**, 60–70.
19 L. Lou, Q. Huang, Y. Lou, J. Lu, B. Hu and Q. Lin, *Chemosphere*, 2019, **228**, 676–684.
20 B. Chen, D. Zhou and L. Zhu, *Environ. Sci. Technol.*, 2008, **42**, 5137–5143.
21 M. Naghdi, M. Taheran, S. K. Brar, A. Kermanshahi-Pour, M. Verma and R. Y. Surampalli, *Sci. Total Environ.*, 2017, **584–585**, 393–401.
22 A. Zille, T. Tzanov, G. M. Gubitz and A. Cavaco-Paulo, *Biotechnol. Lett.*, 2003, **25**, 1473–1477.
23 X. Dong, L. He, H. Hu, N. Liu, S. Gao and Y. Piao, *Chem. Eng. J.*, 2018, **352**, 371–379.
24 X. Xu, X. Cao and L. Zhao, *Chemosphere*, 2013, **92**, 955–961.
25 R. Bourbonnais and M. G. Paice, *FEBS Lett.*, 1990, **267**, 99–102.
26 N. Li, Q. Xia, Y. Li, X. Hou, M. Niu, Q. Ping and H. Xiao, *Polymers*, 2018, **10**, 798.
27 N. Li, Q. Xia, M. Niu, Q. Ping and H. Xiao, *Sci. Rep.*, 2018, **8**, 13947.
28 Y. Zhu, B. Yi, Q. Yuan, Y. Wu, M. Wang and S. Yan, *RSC Adv.*, 2018, **8**, 19917–19929.
29 M. Fu, J. Xing and Z. Ge, *Sci. Total Environ.*, 2019, **651**, 2857–2865.
30 S. Dong, X. Jing, Y. Cao, E. Xia, S. Gao and L. Mao, *Environ. Pollut.*, 2019, **252**, 907–916.
31 J. Lin, Q. Wen, S. Chen, X. Le, X. Zhou and L. Huang, *Int. J. Biol. Macromol.*, 2017, **96**, 377–383.
32 M. Christwardana, *Enzyme Microb. Technol.*, 2017, **106**, 1–10.
33 L. Lonappan, Y. Liu, T. Rouissi, S. K. Brar, M. Verma and R. Y. Surampalli, *Sci. Total Environ.*, 2018, **640–641**, 1251–1258.
34 M. Naghdi, M. Taheran, S. K. Brar, A. Kermanshahi-Pour, M. Verma and R. Y. Surampalli, *Int. J. Biol. Macromol.*, 2018, **115**, 563–571.
35 H.-M. Xu, X.-F. Sun, S.-Y. Wang, C. Song and S.-G. Wang, *Sep. Purif. Technol.*, 2018, **204**, 255–260.
36 H. Zhang, E. Xun, J. Wang, G. Chen, T. Cheng, Z. Wang, T. Ji and L. Wang, *Int. J. Mol. Sci.*, 2012, **13**, 5998–6008.
37 M. Taheran, M. Naghdi, S. K. Brar, E. J. Knystautas, M. Verma and R. Y. Surampalli, *Sci. Total Environ.*, 2017, **605–606**, 315–321.
38 J. Jordaan, S. Mathye, C. Simpson and D. Brady, *Enzyme Microb. Technol.*, 2009, **45**, 432–435.
39 E. Alver and A. Ü. Metin, *Int. Biodeterior. Biodegrad.*, 2017, **125**, 235–242.
40 A. Ü. Metin, *Macromol. Res.*, 2013, **21**, 1145–1152.
41 F. Wang, C. Guo, L. R. Yang and C. Z. Liu, *Bioresour. Technol.*, 2010, **101**, 8931–8935.
42 L. Lonappan, Y. Liu, T. Rouissi, F. Pourcel, S. K. Brar, M. Verma and R. Y. Surampalli, *Chem. Eng. J.*, 2018, **351**, 985–994.

43 M. Cea, M. E. Gonzalez, M. Abarzua and R. Navia, *J. Environ. Manage.*, 2019, **242**, 171–177.
44 O. Saoudi, N. Ghaouar and T. Othman, *Fluid Phase Equilib.*, 2017, **433**, 184–192.
45 C. Qi, X. Liu, C. Lin, H. Zhang, X. Li and J. Ma, *Chem. Eng. J.*, 2017, **315**, 201–209.
46 L. Hongyan, Z. Zexiong, X. Shiwei, X. He, Z. Yinian, L. Haiyun and Y. Zhongsheng, *Chemosphere*, 2019, **224**, 743–750.
47 E. N. de Freitas, G. A. Bubna, T. Brugnari, C. G. Kato, M. Nolli, T. G. Rauen, R. d. F. Peralta Muniz Moreira, R. A. Peralta, A. Bracht, C. G. M. de Souza and R. M. Peralta, *Chem. Eng. J.*, 2017, **330**, 1361–1369.
48 P. Galliker, G. Hommes, D. Schlosser, P. F. Corvini and P. Shahgaldian, *J. Colloid Interface Sci.*, 2010, **349**, 98–105.
49 F. R. Caetano, E. A. Carneiro, D. Agustini, L. C. S. Figueiredo-Filho, C. E. Banks, M. F. Bergamini and L. H. Marcolino-Junior, *Biosens. Bioelectron.*, 2018, **99**, 382–388.